A NEW MARTIAN PALAEOPRESSURE CONSTRAINT BEFORE 4 GA FROM CRATER SIZE-FREQUENCY DISTRIBUTIONS IN MAWRTH VALLIS. A. O. Warren[1] and E. S. Kite[1], [1]University of Chicago, Department of Geophysical Sciences (aowarren@uchicago.edu).

Introduction: Changes in Martian atmospheric pressure over time are an important control on Mars' climate evolution. Most constraints for Martian atmospheric pressure over time are indirect. A direct method uses minimum crater size to estimate an upper limit on atmospheric pressure [1,2]. Thin planetary atmospheres enable smaller objects to reach the surface at high velocities, forming craters. The Mawrth Vallis region contains the oldest known hydrously altered sedimentary rocks in the Solar System, overlying a paleosurface with a high density of preserved ancient embedded craters. These are identified as craters that are visibly embedded in the >4 Ga stratigraphy. Using high-resolution images, anaglyphs and digital terrain models (DTMs), we compared the size-frequency distribution of these craters to models of atmospheric filtering of impactors to obtain a paleopressure estimate of 1.0±0.1 bars. We use this alongside other existing data and estimates to constrain a basic 2-component, process-agnostic atmospheric evolution model.

Geological context & crater identification: The Noachian phyllosilicates northwest of Oyama crater are thick, finely layered sedimentary deposits. Hydrous clay minerals [3] make them of interest for constraining the atmospheric pressure during the Early Noachian, when liquid water must have been present for alteration to occur. Additionally, they trap an even more ancient crater population at their base on a 'dark paleosurface' [4]. These craters are infilled with layered phyllosilicates and therefore must pre-date phyllosilicate deposition [5]. The preservation of >100m diameter craters on this paleosurface shows that it was exposed long enough to be impacted by bolides [4]. Stratigraphic relationships [5] and cratering ages for the overlying phyllosilicate units give an age for the heavily cratered paleosurface of >4 Gyr. Ancient embedded craters (e.g. Fig 1) were identified using the following criteria: (1) Approximately circular topographic depression (2) depth << 0.2 × diameter, (3) minimum 150° arc of of elevated rim preserved, rim may be discontinuous, (4) <50% of depression obscured by sand infill, center of crater must always be sand free, (5) feature is concave-up in anaglyph. Features that met at least (1), (2) and (4) were counted separately as candidate craters. Additional support for a crater being ancient and embedded includes disk-shaped, layered sedimentary deposits inside the crater. Ellipses were fit to points marked on crater rims in ArcGIS in order to measure their diameter.

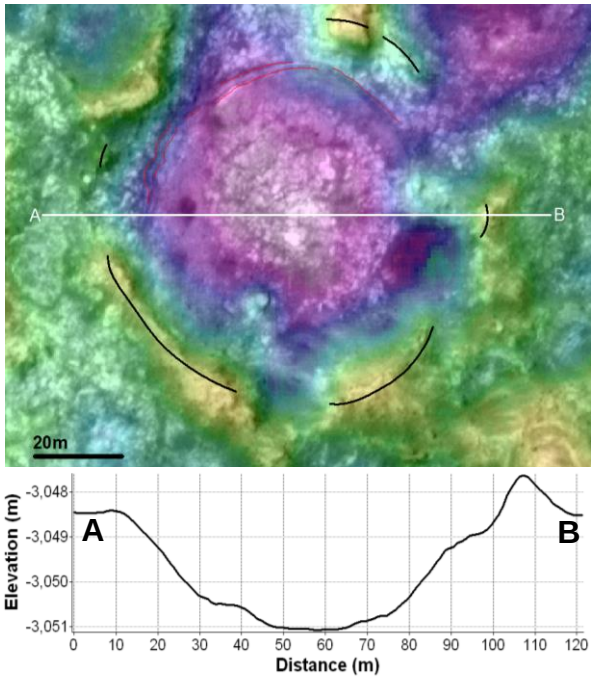

Figure 1: Example embedded crater with cross section. Bold black lines denote identified crater rim. Colors show elevation relative to Mars geoid (orange: -3045m, white: -3051m).

Atmospheric filtering model & preliminary results: Synthetic crater populations were created using a forward model of impactor-atmosphere interactions modified from [6,7] by [2] for impactors with specified size [8] and velocity [9] distributions, and proportion of different impactor densities and strengths (i.e. irons, chondrites etc.) [10]. Paleopressure is estimated by treating impacts as a Poisson process and bayesian fitting of the observed size-frequency distribution to the model distributions. Our preliminary result of 1.0±0.1 bar from definite embedded craters (0.4±0.1 bars with candidates) is consistent with estimates from prehnite stability (3 – see Fig 2 for constraint numbering) [2], conditions for carbonate formation (5), [11] and modelling based on Ar isotope ratios in Allan Hills 84001 (2a) [12] in suggesting that atmospheric pressure before 4 Ga was $\lesssim$1.5 bar (Fig 2). The likelihood of intersecting a crater on an erosion surface through a 3D volume filled with randomly distributed craters is proportional to crater diameter [2]. We include this effect in our estimate by using a fractal correction. Erosion and sedimentation processes may contribute to the preferential removal of small craters. Any correction for these effects would lower our paleopressure estimate, which strengthens the case for a lower atmospheric pressure early in Mars' history. Without cratering ages for the 'dark paleosurface' itself, it is possible that it predates the layered phyllosilicates by hundreds of millions of years. This is motivation to search for additional em-

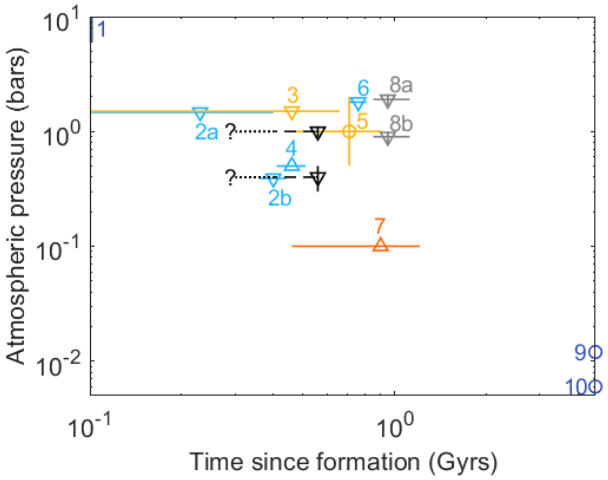

Figure 2: Mars paleopressure constraints (modified from [2]). Direction of triangles indicates upper/lower bound. 1 – cosmochemical estimate [13]. Black symbols – this study, light blue - isotope-based models (2 [12], 4 [14], 6 [15]) yellow – mineralogical/thermodynamic constraints (3 [2], 5 [11]), grey – crater counting studies (8 [2]), orange - Gusev bomb sag (7 [16]. 9 & 10 are modern CO_2 inventory with and without contributions from CO_2 icecaps respectively.

bedded crater populations higher in the Mawrth stratigraphy. Our estimate suggests that at some point earlier than 4 Ga Mars' atmospheric pressure must have fallen to 1.0±0.1 bar or below for long enough to accumulate the observed embedded crater population. This could be evidence for early escape of much of Mars' primary atmosphere, as suggested by the high $^{129}Xe/^{132}Xe$ ratio of the present atmosphere [17]. This is evidence against the hypothesis that a warm and wet early Mars can be explained by retention of a thick, H_2-rich proto-atmosphere[18].

2-component atmospheric evolution model: The atmospheric evolution of Mars depends on the relative contributions of source and sink terms over time. Detailed evolution models rely on balancing fluxes from processes such as impact delivery/erosion, outgassing, and loss to space, for which many assumptions are necessary. We used a basic 2-component model working backwards from observed modern atmospheric pressure (12 mbar if CO_2 ice caps are included [19]) and measured MAVEN loss rates [20], gathering sources and sinks into 1 term each. We choose to express these terms as either a powerlaw ($\Delta P_{source/sink} = k_{1/3}*t^{(-k_{2/4})}$) or an exponential ($\Delta P_{source/sink} = k_{1/3}*\exp(-t/k_{2/4})$) with free parameters k_1, k_2 (sinks), k_3 & k_4 (sources), giving 4 possible source-sink set-ups (Fig 3). The parameters $\{k_1, k_2, \ldots k_4\}$ are found using the upper limits of existing paleopressure estimates (excluding 2b, 4 & 8b – Fig 2) as hard constraints to limit permitted pressure histories. The values of the parameters themselves are perhaps less important than the array of possible pressure evolutions (Fig 3). Existing data – including this study – cannot rule out pressure histories that start with negligible atmospheres as late as 4.1 Ga, nor those that experience atmospheric collapse (i.e. have permanent ice caps) between ~3.6 Ga and just before present .

Acknowledgements: J.-P. Williams wrote the model of impactor-atmosphere interactions. J. Sneed produced the HiRISE DTMs using the pipeline of [21]. Grants: NASA (NNX16AJ38G).

References: [1] Vasavada A. R. et al. (1993) *JGR Planets, 98*, 3469-3479. [2] Kite E. et al. (2014) *Nature Geoscience, 7*, 335-339. [3] Bishop J. L. et al. (2008) *Science, 321(5890)*, 830-833. [4] Loizeau D. et al. (2010) *Icarus, 205*, 396-418. [5] Loizeau D. et al. (2012) *Planet. Space Sci. , 72(1)*, 31-43. [6] Williams J. P. et al. (2014) *Icarus, 235*, 23-36. [7] Williams J. P. & Pathare A. V. (2017) *Meteoritics & Planetary Sci., 53(4)*, 554-582. [8] Brown P. et al. (2002) *Nature, 420*, 294-296. [9] Davis P. (1993) *Icarus, 225*, 506-516. [10] Ceplecha Z. et al. (1998) *Space Sci Rev., 84*, 327-341 [11] Van Berk W. et al. (2012) *J. Geophys. Res., 117*. [12] Cassata W. (2012) *Earth and Planet. Sci. Letters, 479*, 322-329. [13] Lammer et al. (2013) *Space Sci. Rev., 174(1-4)*, 113-154. [14] Kurokawa et al. (2018) *Icarus, 299*, 443-459. [15] Hu et al. (2015) *Nature Comm., 6*:10003 [16] Manga et al. (2012) *Geophys. Res. Lett., 39*. [17] Conrad P. (2016) *Earth Planet. Sci. Lett., 454*, 1-9. [18] Saito H. & Kuramoto K. (2018) *Monthly Notices of the Royal Astronomical Soc., 475(1)*, 1274-1287. [19] Bierson C.J. et al. (2016) *Geophys. Res. Lett., 9*, 4172-4179. [20] Lillis R. et al. 2017 *Space Sci. Rev., 195*, 357-422. [21] Mayer D.P. & Kite E.S. (2016) *LPSC XLVII*, abstract #1241.

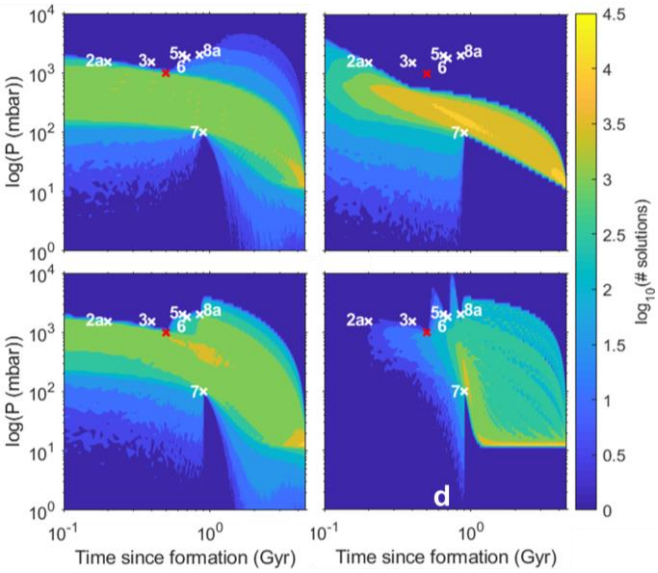

Figure 3: Density of possible pressure evolution tracks for four possible 2 component set-ups (constraints correspond to Fig 2, red 'x' – this study). a) exponential source, exponential sink, b) powerlaw source, exponential sink, c) exponential source, powerlaw sink, d) powerlaw source, powerlaw sink.